

Tsunami Detection Techniques

Sanjay V. Khobragade¹, Nikita Gosavi¹, Urmila S. Khobragade²

*1. Dr. B. A. T. University Raigad, (MH) India, svk_2305@yahoo.co.in
Mobile: 09421900190, +912140275212, Fax: +912140275142
2. Atmiya Vidya Mandir, Kamrej Surat, Gujrat*

Abstract

The earthquake occurs in Indonesia on December 26, 2004 is of the magnitude of 9.0 - 9.2. The epicenter located about 300 km west of Medan which killed a millions of people, in Indonesia, Sri Lanka, and India. Recent technological and theoretical developments suggest that its effectiveness could be greatly increased through the use of satellite communications, automatic data acquisition and transmission, and computerized pre calculation of wave effects.

This Paper summarizes the different theoretical Tsunami detection and measurement techniques to provide critical information that may have used for various future activities and subsequent recovery activities.

1. Introduction

A Tsunami is a series of waves with a longer wavelength and period as well. Tsunamis are generated by any large, impulsive displacement of the sea bed level. Earthquakes generate tsunamis by vertical movement of the sea floor. Earthquakes of $M > 6.5$ (Richter scale) are critical for tsunami generation. Tsunamis are also triggered by landslides into or under the water surface, and can be generated by volcanic activity and meteorite impacts [1].

Velocity of tsunami is dependent on the depth of water through which it travels $V = \sqrt{g \cdot h}$ where h is the water depth and g is gravitational acceleration. Tsunamis travel approximately 700 kmph in 4000 m depth of sea water. In 10 m of water depth the velocity drops to about 36 kmph. Tsunamis range in size from centimeters to over 30 m height. Most tsunamis are less than 3 m in height and In deep water it may be greater than 200 m.

2. Detection Methods

Following are the methods discussed in details.

2.1 Acoustic Detection

Acoustic waves can serve as tool for the diagnosis of ocean processes. The main physical factor influencing sound propagation is the travel time of the acoustic signal. Thus, measurements of signal travel time can identify water movements. The method are based on the M-sequence, which is a long series of pulses with phase modulation allow the compression of the signals in time by correlation processing [2].

2.1.1 Signal Processing Technique for Acoustic Detection

The correlation function of the signal, calculated on an interval equal to the length of the sequence, represents a tone-pulse with a triangle-shape envelope with the basis equal to the double length of the M-sequence (eq. 1):

$$R(\tau) = \begin{cases} (2^n - 1) \cdot \left(1 - \frac{|\tau|}{\tau_0}\right) \cos(\omega_0 \tau), & |\tau| \leq \tau_0, \\ 0, & |\tau| > \tau_0. \end{cases} \quad (1)$$

For measurement, the variations of the travel time of the received signal were divided into intervals equal to one M-sequence. For each k -th interval the mutual correlation (τ) k R with a replica was estimated as (eq. 2):

$$R_k(\tau) = \int_{t_k}^{t_k+T} y_k(t)M(\tau-t)dt, \quad (2)$$

Where $R_k(\tau)$ is the estimation of the pulse response of the system, $M(t)$ is the replica of the radiated signal, T is the length of the M-sequence, $y_k(t)$ is the k -th sample of the received signal. Presenting(eq. 3):

$$R_k(\tau) \text{ as } R_k(\tau) = h_k(\tau) \exp(i\omega_0 \tau_k) \quad (3)$$

as a pulse response of the system shifted in time by τ_k , we can introduce function $\rho_k(m)$ as(eq. 4):

$$\rho_k(m) = \int_{\tau} R_k(\tau) \cdot R_{k+m}^*(\tau) d\tau = e^{i\omega_0(\tau_k - \tau_{k+m})} \int_{\tau} h_k(\tau) h_{k+m}^*(\tau) d\tau, \quad (4)$$

Where $|\rho_k(m)| = \int_{\tau} h_k(\tau) h_{k+m}^*(\tau) d\tau$ is the amplitude of the function $\rho_k(m)$ and $\phi_k(m) = \omega_0(\tau_k - \tau_{k+m})$ is the phase. To increase the accuracy of the estimation of $\rho_k(m)$ we made the following averaging(eq. 5):

$$\hat{\rho}_k(m) = \frac{1}{M-1} \sum_{i=k}^{k+M} \rho_i(m). \quad (5)$$

2.2 Paris Concept

Current ideas for a space-based PARIS sensor envisage the antenna having 12 independently tracking beams. This means that coverage of the world's oceans is already improved by a factor of 12, compared to a conventional altimeter, for a single instrument. An important feature for tsunami detection is assured continuous improvement in capabilities (transmitted power, bandwidth and frequencies) [3].

2.2.1 PARIS Airborne Demonstrations

For airborne demonstration a flight is carried out in Spain on 25 September 2001, In the region of the Mediterranean Sea, a trench in the sea floor disturbs the water current and produces a 30 cm dip about 100km long in the mean sea level. The amplitude and wavelength of such a topographic feature are similar to those of a tsunami in Open Ocean.

Several GPS-buoys were deployed to provide some ground truth points. GPS stations were installed at several places along the coast as well, and kinematic differential GPS was used to retrieve the plane's trajectory. The C/A code was processed by IEEC, whereas the encrypted P-code (Y-code) processing was done by JPL-NASA for IEEC. Valid data was recorded for the full path when flying north. The Palamos Canyon 30cm dip is observed in both C/A and P-code derived profiles. The same flight was repeated one year later, on 27 September 2002, using the same PARIS altimeter over an extended track, using a fully independent data processor. Only the C/A code was processed. The retrieved profile looks very similar to the one obtained in PARIS-alpha showing the robustness of the PARIS technique. The key issue of the system is real time on-board processing and data downlink [3].

2.3 Wavelet analysis of Seismogram

Wavelet techniques are intrinsically better suited to the analysis of transient signals such as seismograms. The wavelet analysis discussed in this paper employed application of the Continuous Wavelet Transform (CWT) using the Daubechies-4 ("db4") wavelet. This appeared effective at identifying features in seismic data. The CWT is defined as the sum over all time of the signal $f(t)$ multiplied by scaled, shifted versions of the wavelet function ψ . The wavelet transform C is then given by (eq. 6),

$$C(\text{scale}, \text{position}) = \int_{-\infty}^{\infty} f(t)\psi(\text{scale}, \text{position}, t)dt \quad (6)$$

This refers to position in time with respect to the signal $f(t)$. Since signals are finite, the integration limits become the size of the signal. The WT can simultaneously achieve: (1) Accurate frequency representation for low frequencies, and (2) Good time resolution for high frequencies. For tsunami warning purposes, the very long period wave was found to show up most strongly over this period range.

The WT operates by scaling the wavelet to different periods and then correlating the scaled wavelet along the duration of the signal. As this correlation occurs, the wavelet would go in and out of phase with a pure sinusoid. This oscillation produces the ripple-like effect which is characteristic of the WT [4].

2.4 Tsunami Waveform Inversion

Satake shows, for the first time that the inversion of tide-gage records can be used to retrieve some information about the tsunamigenic source mechanism. In Satake's approach, it is necessary to preliminarily assume a fault plane solution, then, segmenting the fault plane into several sub-faults. This method allows for the estimation of the slip distribution along the fault [5].

2.4.1 Inversion Method

The forward model for the tsunami propagation, i.e. for the calculation of the synthetic tide-gage records starting from an initial water elevation field, is based on the linear shallow water equations (eq. 7):

$$\begin{aligned}\partial_t \zeta &= -\nabla \cdot (h\mathbf{v}) \\ \partial_t \mathbf{v} &= -g\nabla \zeta,\end{aligned}\quad (7)$$

completed by the following boundary conditions (eq. 8):

$$\begin{aligned}\mathbf{v} \cdot \mathbf{n} &= \frac{g}{c} \zeta && \text{on the open boundary} \\ \mathbf{v} \cdot \mathbf{n} &= 0 && \text{on the solid boundary.}\end{aligned}\quad (8)$$

Where $\mathbf{v} = (u, v)$ is the horizontal fluid velocity vector, h is the basin depth, g is the gravity acceleration, $c = 1/2(gh)$ is the wave phase speed and \mathbf{n} is the unit vector, outwardly directed, normal to the boundary. To solve Eqs. Author use a finite-element technique, finite-element spatial discretisation transforms Eqs. (7) and (8) as (eq. 9):

$$\frac{d}{dt} \xi(t) = A \xi(t). \quad (9)$$

3N-components vector representing the value of the unknown fields on the nodes of the finite element grid consisting of N nodes and A is a matrix of constant coefficients that also includes the boundary conditions. Formal solution for the unknown vector through a spectral decomposition of the matrix A (eq. 10):

$$\begin{aligned}\xi(t_k) &= \exp [A(t_k - t_0)] \xi(t_0) = \\ &= \text{Exp} [\Lambda(t_k - t_0)] E^{-1} \xi(t_0),\end{aligned}\quad (10)$$

Where $\xi(t_k)$ is the unknown vector computed at the time t_k , E and E^{-1} are, respectively, the eigenvectors matrix and its inverse, whereas Λ is the diagonal eigenvalues matrix and $\xi(t_0)$ is the initial condition. Green's function of the problem as (eq. 11):

$$G_{kj}^i = E_{in} \exp [\Lambda_{nm}(t_k - t_0)] E_{mj}^{-1}, \quad (11)$$

Where the rule of summation on the repeated index is adopted, If we restrict the problem to the case of a static initial condition and to the calculation of the water elevation solely, the forward problem can be written in terms of the Green's functions as:

$$\zeta_i(t_k) = G_{kj}^i \zeta_j(t_0). \quad (12)$$

$\zeta_i(t_k)$ is the elevation computed at the i -th node at the time t_k and the Green's function G_{ki}^i has the usual interpretation [5]

2.5 Tsunami Detection using Hydrolevelling

Three Hydrolevelling sensors are placed to measure reactor shaft tilt vector. The optoelectronic sensor in system of connected vessels consists of a flat window cell made of a metal frame with optical glass and an optoelectronic system for hydrostatic liquid level measurement. This optoelectronic part is based on a CCD line image sensor. The sensors are interconnected by hydraulic and pneumatic pipes. Liquid temperature in sensors is measured by means of thermometers built in the sensors. This temperature is used for measured data correction influenced by liquid temperature dilatation. The liquid levels in individual vessels lie in one horizontal plane when certain physical conditions are fulfilled. This plane can then serve as the reference plane for the height differences (elevations) between the individual points' measurement. The range of height difference measurement is ± 10 mm; measuring precision is 0.01 mm as shown in figure 1.

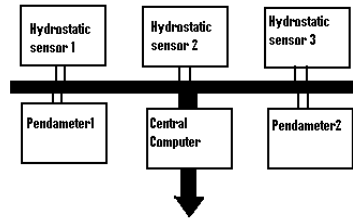


Figure No. 1 Experimental set up for tsunami detection

The Pendametric method uses the properties of a vertically damped pendulum. Its hinging point is connected to the measured object. The position of the pendulum wire is measured biaxially in a reference plane which is usually horizontal. The wire's position in the reference plane and its length determines the reactor shaft tilt. The optoelectronic method is used for this position measurement such as in the hydrolevelling method. The measuring range of the pendameter wire position is ± 2 mm in both coordinate axes; the resolution is 0,001 mm. Figure shows the both hydrolevelling and pendametric sensors installed on the reactor shaft [6].

3. Present Tsunami Warning System

Several alternatives TWS are suggested as:

Air Pulse Detection Analysis: Destructive tsunamis involve such large scale vertical sea floor dislocations that a detectable air pulse (atmospheric tsunami) is also generated. Early analysis of such air pulses might permit a quantitative estimate of tsunami magnitude. *Tide Gage Calibration:* It is well known that different tsunami records made at the same location exhibit many similarities. Therefore, it may be possible to calibrate selected individual gages in terms of relative spectral sensitivity. As a prediction aid for warning purposes, correlation of many such record spectra with such factors as epicenter distance and coastal orientation at source, coupled with analysis of dispersion and spreading, might lead to sensitivity indices that could be rapidly applied and interpreted in terms of relative effects elsewhere. *Direct Seismic Method:* Based on the historical records and geophysical evidence, one could define all likely tsunami source regions in the Pacific and install autonomous, passive event recorders at selected locations.

4. Conclusion

This paper I based on the study of different tsunami detection techniques available. There are hundreds of methods available we tried to explain some of prominent methods.

5. References

1. "Preventive / Protection and Mitigation from risk of Tsunami", A Strategy Paper, 2005, A Ministry of Home Affair, Government of India.
2. A. Stromkov, I. N. Didenkulov, Ya. S. Karlik, Pelinovsky Petropavlovsk -Kamchatski, "Acoustic Detection of Tsunamis in the Open Sea". Tsunami Workshop, Pp 55- 62, September 10-15, 2002.
3. M. Martin-Neira, C. Buck, The Netherlands, S. Gleason, M. Unwin, M. Caparrini, E. Farr'es, Olivier Germain, G. Ruffini, F. Soulat, "Tsunami Detection Using the PARIS Concept", Progress In Electromagnetics Research Symposium 2005, Hangzhou, China, August 22-26.
4. Oliver G. Lockwood (primary author) Pembroke College, Cambridge University, "Wavelet Analysis of the Seismograms of the 2004 Sumatra-Andaman Earthquake and its Application to Tsunami Early Warning" CB2 1RF, United Kingdom Hiroo Kanamori, Seismological Laboratory, California Institute of Technology, Pasadena, CA 91125, U.S.A.
5. A. Piatanesi, S. Tinti, and G. Pagnoni Dipartimento di Fisica, Universit'a di Bologna, Bologna, "Tsunami waveform inversion by numerical finite-elements Green's functions" Italy Received: 06 August 2001 – Accepted: 16 November 2001, Natural Hazards and Earth System Sciences (2001) 1: 187–194 c European Geophysical Society 2001.
6. Lubomír Ondříš, Viktor Rusina, Ján Buzási, Marian Trutz, "Tsunami earthquake detected in the nuclear power plant" Institute of Measurement Science, Slovak Academy of Sciences Bratislava, Slovakia MEASUREMENT SCIENCE REVIEW, Volume 6, Section 3, No. 3, 2006.